The modelling and design of an MRI-compatible cryosurgical probe

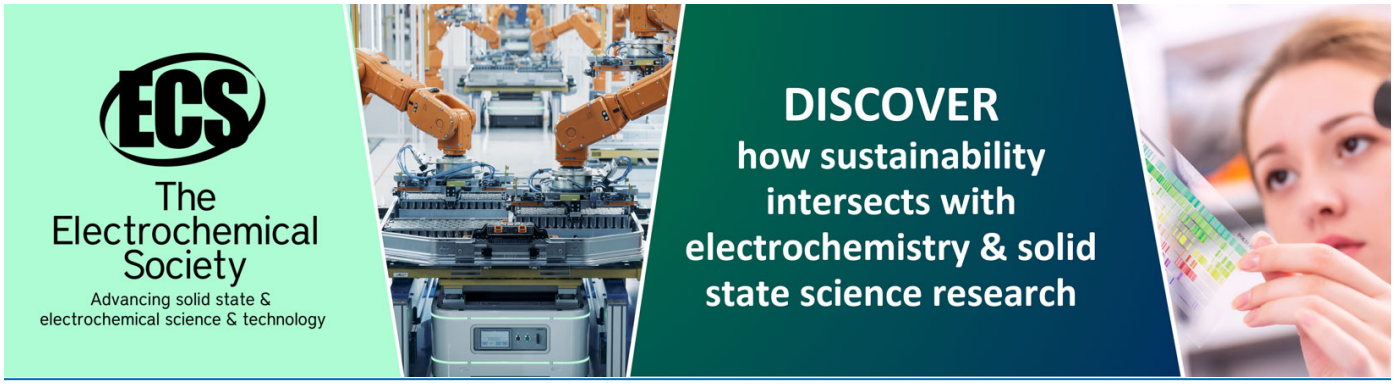

The modelling and design of an MRI-compatible cryosurgical probe

L Kossel[1], J Pfotenhauer[1], and R Harter[2]

[1]University of Wisconsin-Madison, Department of Mechanical Engineering
Madison, WI 53706, USA
[2]Marvel MedTech LLC, Madison WI 53562, USA

Email: lkossel@wisc.edu

Abstract. Cryo-ablation is a breast cancer treatment method that utilizes a small probe in precise locations within the body to freeze and destroy unwanted cancer tissue. Recently, there has been a growing interest in combining cryo-ablation with magnetic resonance imaging (MRI). The challenge of combining these two technologies is that MRI devices require the absence of metals, and traditional heat exchangers used in cryoprobes are typically composed of thermally conductive metals that tend to disrupt the image produced by an MRI, impairing its functionality. Subsequently, it becomes of interest to develop a heat exchanger composed of thermally conductive MRI-compatible materials such as zirconium. This report presents the results of a thermal modelling effort to characterize and design a non-metallic Joule-Thomson cryoprobe for cryo-ablation. The model is comprised of a Joule-Thomson valve, as well as a discretized recuperative heat exchanger that includes the effects of axial conduction, pressure drop, two-phase and single-phase convection correlations, and fluid properties for single-components and mixtures. The device operates at 170 K with a heat load of 10 W, which is a viable temperature and heat load for cryo-ablation.

1. Background

Cryo-ablation has been used to successfully treat breast cancer patients for the past two decades. However, there is new interest in pairing cryosurgical technology with magnetic resonance imaging (MRI). Currently, X-ray mammography is the most common imaging technique for detecting breast cancer, and, despite being the most common, it has a 60% lower tumor sensitivity rate when compared to MRI [1]. Thus, pairing MRI with cryosurgery could potentially result in a more effective method of treating breast cancer. The challenge of combing these two technologies is that MRIs require the absence of both ferromagnetic and non-ferromagnetic metals as to not interfere with the imaging process used by the MRI to detect tumors properly. Traditionally, the heat exchangers in the cryoprobes used for cryo-ablation are composed of high conductivity metals that tend to disrupt the image produced by the MRI. It then becomes of interest to develop both the heat exchanger, and indeed the entire cryosurgical probe out of non-metallic, yet high thermal conductivity, MRI-compatible materials, such as zirconium or silicon. Although some polymers such as polyethylene could also be compatible for this application, most polymers exhibit inferior thermal properties when contrasted with the ceramics of interest.

2. Thermodynamic modelling

The numerical model described in this paper utilizes the Engineering Equation Solver software (EES) [2], which simplifies iteration and includes various thermodynamic functions. The model makes extensive use of iteration and guess-values for unknown parameters in order to iteratively solve for them at a later time. Some examples of this process include guessing the pressure to find intermediate fluid properties, and guessing the length of the heat exchanger in order to determine a radial flow resistance. Both parameters require iteration in order to determine the true values. Similarly, fluid properties and convection correlations for single-component gases from EES were used in early adaptations of the model, which yielded results that were necessary to ultimately develop a mixed-gas model.

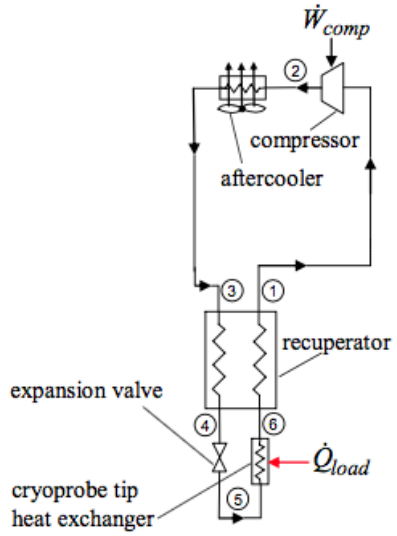

Figure 1. A schematic of a Joule-Thomson cryosurgical probe [3].

2.1. Miniature mixed-gas Joule-Thomson systems

A typical cryosurgical probe achieves cooling by utilizing the Joule-Thomson effect, where the working fluid undergoes an isenthalpic expansion through a throttle valve that can drop the fluid temperature significantly. In the case of a cryosurgical probe, the heat load represents the heat leaving the tissue with which the probe is in contact, thereby producing the required tissue freezing. The advantages of using a gas mixture for the JT cycle, especially being able to achieve significant cooling at a relatively low pressure ratio, is an important safety feature for the cryo-ablation application. Figure 1 shows the schematic for a simple Joule-Thomson System, which includes a compressor, heat exchanger, aftercooler, expansion valve, and heat load. The heat load picked up from the tissue is determined using equation (1).

$$\dot{q}_{\text{load}} = \dot{m}(h_1 - h_3) \tag{1}$$

The model investigated in the present report uses an open cycle cryocooler in which the compressed gas vents to ambient air. The cycle therefore excludes the compressor and aftercooler shown in Figure 2. The low side pressure of the heat exchanger is at atmospheric pressure, while the high side pressure is set at 2 MPa. The desired cooling of the model is 10 W at 170 K, which is a viable temperature and heat load for cryo-ablation [4].

2.2. Gas mixture properties

Selecting the appropriate gas mixture for a Joule-Thomson system is important, as it dictates the temperature and heat load picked up at the cryoprobe tip. The gas mixture optimization described by Detlor et. al. [5,6] was used to determine the optimal three-component mixture that results in the highest minimum value of the isothermal enthalpy change over the desired temperature range and pressure drop. Table 1 presents the gas optimization parameters and results.

The first mixture, $0.6C_3H_8 + 0.36CH_4 + 0.04N_2$, provides the highest minimum value of the isothermal enthalpy change, and is therefore the mixture used in the numerical model. REFPROP includes a number of regions where property data is undefined. In order to bypass these, and the associated numerical problems, we have adopted an approach wherein the values that are available from REFPROP are used to populate tables (one for each pressure: 0.1, 0.5, 1.0, 1.5, 2.0 MPa) for temperatures ranging from 150 K to 300 K. An interpolation technique is subsequently used to extract the desired property data for any pressure and temperature within the range covered by the tables.

Table 1. The results of the gas mixture optimization, which include the gas mixtures that result in the largest minimum isothermal enthalpy change

Optimization Input Parameters	
P_{in} = 2 MPa	$T_{\text{h,in}}$ = 293 K
P_{out} = 0.1 MPa	T_{load} = 170 K
Input Gases: Methane (CH_4), Ethane (C_2H_6), Propane (C_3H_8), and Nitrogen (N_2)	
Optimized Gas Mixtures	
$0.6C_3H_8 + 0.36CH_4 + 0.04N_2$	Δh_T = 1468 J/kg
$0.72C_2H_6 + 0.18CH_4 + 0.1N_2$	Δh_T = 708.78 J/kg
$0.48N_2 + 0.32C_2H_6 + 0.2C_3H_8$	Δh_T = 510.03 J/kg

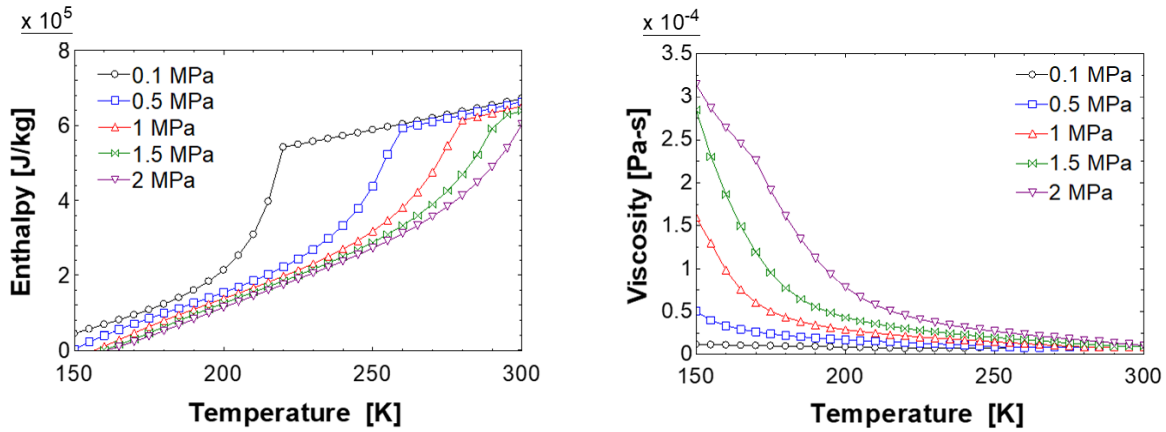

(a) (b)

Figure 2. The (a) specific enthalpy and (b) viscosity property data for the optimized gas mixture. Many other properties were also used in the numerical model's calculations.

2.3. Heat exchanger discretisation

The most engaging component of a Joule-Thomson system for a cryosurgical probe is the recuperative heat exchanger, which dictates the overall performance of the system, including the allowable heat load. As fluid flows through the heat exchanger, fluid properties such as specific heat and thermal conductivity change quickly as a result of the pressure drop and rapid temperature change. In order to account for these changes, the heat exchanger model is discretised, as shown schematically in Figure 3.

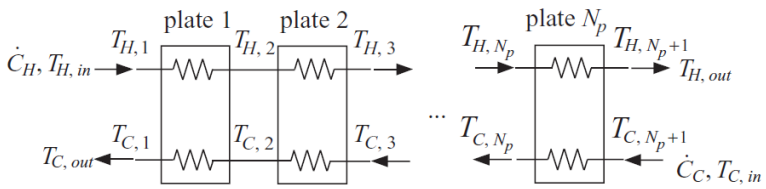

Figure 3. The counter-flow heat exchanger discretisation schematic, where each section represents an equal heat flow. Note that since heat transfer is the basis of discretisation, the size of each sub-heat exchanger varies, and is indirectly determined [8].

The discretisation process splits up the heat exchanger into any number of desired sub-heat exchangers, which are defined as having an equal amount of heat flow from the hot fluid to the cold fluid. This technique results in a more accurate representation of fluid behavior inside the heat exchanger. Before discretisation, initial parameters of the inlet and outlet conditions of the entire heat exchanger are used to determine the overall required heat exchanger effectiveness.

$$\varepsilon = \frac{\dot{m}(h_{\mathrm{h,in}} - h_{\mathrm{h,out}})}{\dot{m}(h_{\mathrm{h,in,ideal}} - h_{\mathrm{c,in}})} \tag{2}$$

The numerator of equation (2) is the total heat transferred by the heat exchanger, which can be used to discretise the heat exchanger into N sections of equal heat flow.

$$\dot{q} = \dot{m}(h_{\mathrm{h,in}} - h_{\mathrm{h,out}}) \tag{3}$$

$$\dot{q}_{\mathrm{d}} = \frac{\dot{q}}{N} \tag{4}$$

The discretised heat flow is then used to determine fluid enthalpy for each sub-heat exchanger with a counter-flow configuration:

$$h_{\mathrm{h},i+1} = h_{\mathrm{h},i} - \frac{\dot{q}_{\mathrm{d}}}{\dot{m}} \tag{5}$$

$$h_{\mathrm{c},i+1} = h_{\mathrm{c},i} - \frac{\dot{q}_{\mathrm{d}}}{\dot{m}} \tag{6}$$

This creates the enthalpy profile of each side of the heat exchanger which, along with the varying pressure, can then be used to determine the temperature of the fluid for each sub-heat exchanger. Furthermore, any combination of two of these three properties can then be used to determine the rest of the fluid properties of interest for every sub-heat exchanger, including thermal conductivity, viscosity, and specific heat. Additionally, since the pressure drop is not yet known at this point, it is necessary to assume a pressure and iterate for the true pressure once the internal flow convection correlations have been included.

2.4. Length iteration

Heat exchanger discretisation is based on sections of equal heat transfer, which does not guarantee equal sub-heat exchanger size. Specifying internal flow convection correlations, the counter-flow ε-NTU relationship, and the thermal resistance of radial heat transfer allows for the length of each sub-heat exchanger, and therefore the length of the entire heat exchanger, to be determined.

With single-component fluids, it is preferable to use the convection correlations and heat exchanger functions that are built into EES; however, these built-in functions are incompatible with the technique this model uses to determine gas mixture properties. Instead, a series of custom EES functions were constructed that determine the phase of the fluid at each increment and apply the appropriate set of correlations to find the heat transfer coefficient and pressure drop through each sub-heat exchanger. The flow type and associated correlations are summarized in Table 2 [9-13].

Table 2. The heat transfer coefficient and pressure drop correlations used for the flow patterns that appear in the heat exchanger [9-13].

	Heat Transfer Coefficient Correlation	Pressure Drop Correlation
Single-Phase	Gnielinski (1976)	Zigrang and Sylvester (1982)
Two-Phase Boiling	Shah (1982)	Ould Didi et al. (2002)
Two-Phase Condensation	Dobson and Chato (1998)	Ould Didi et al. (2002)

Once the pressure drop at each increment is known, it is possible to find the true properties values through iteration. Also, once the appropriate heat transfer coefficients are determined, the total resistance to radial heat flow can be calculated

$$R_{\mathrm{conv},i} = \frac{1}{\bar{h}A_{\mathrm{c}}} \tag{7}$$

$$R_{\mathrm{cond},i} = \frac{\ln\left(\frac{D_{\mathrm{o,wall}}}{D_{\mathrm{i,wall}}}\right)}{2\pi k_{\mathrm{zr},i}L_i} \tag{8}$$

$$R_{\mathrm{total},i} = R_{\mathrm{conv,h},i} + R_{\mathrm{conv,c},i} + R_{\mathrm{cond},i} = \frac{1}{UA_i} \tag{9}$$

Consequently, equating the conductance derived from the radial heat flow resistance to the conductance associated with the counter-flow ε-NTU equation enables the model to iteratively determine the length of each sub-heat exchanger, and therefore the length of the entire heat exchanger.

2.5. Axial conduction

Axial conduction through the heat exchanger is taken into consideration using an axial conduction parameter γ for each sub-heat exchanger. An axial conduction resistance is first calculated as a simple plane wall, and the axial conduction parameter is determined.

$$R_{\mathrm{ac},i} = \frac{L_i}{k_{\mathrm{zr},i}A_{\mathrm{c}}} \tag{10}$$

$$\gamma_i = \frac{1}{R_{\mathrm{ac},i}\dot{C}_{\mathrm{min},i}} \tag{11}$$

$$\varepsilon_{\mathrm{ac},i} = \varepsilon_{\mathrm{nac},i} - \gamma_i \tag{12}$$

For this model, the low$-\gamma$ option is used since the value of γ is much less than unity for each sub-heat exchanger [8]. Including the axial conduction parameter results in an adjusted heat exchanger efficiency to be used in the ε-NTU relationship. Although the modified heat exchanger effectiveness results in a less effective, and therefore larger, recuperator it is a more accurate representation of heat exchanger performance for the model.

2.6. Geometry and material considerations

Although the helical tube-in-tube geometry used in this model results in a reasonable heat exchanger size, improvements upon the heat exchanger geometry can be made to further decrease its calculated size. Potential improvements include adding various fin arrangements on both sides of the fluid flow, or implementing perforated plates instead of tubes.

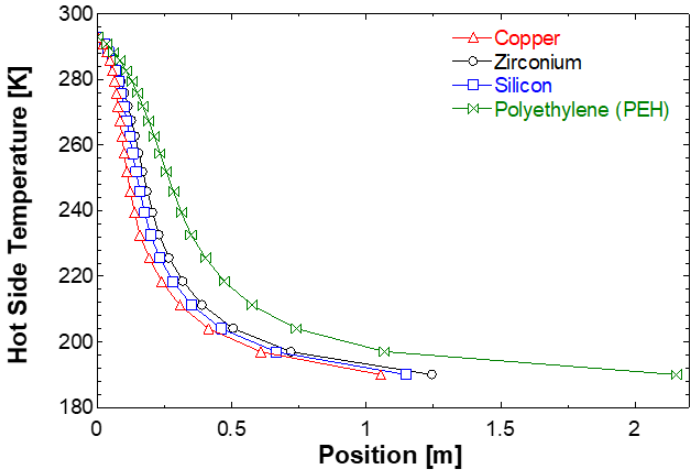

Figure 4. The required heat exchanger length for a hot side cool-down to 190 K for copper, zirconium, silicon and high-density polyethylene. Copper is a common heat exchanger material, silicon and zirconium are MRI-compatible thermally conductive ceramics, and polyethylene is an MRI-compatible polymer with low thermal conductivity.

Although zirconium is used in this model, there are other thermally conductive ceramics that could be used, such as silicon. Figure 4 shows the heat exchanger length required for the hot side of the heat exchanger to reach 190 K for various materials, which suggests that for the geometry used in this model, materials with high thermal conductivity are desired to limit the length of the heat exchanger.

3. Results

The parameters and results of a helical tube-in-tube heat exchanger simulation using this numerical model are presented in Table 3:

Table 3. The input parameters and results of the numerical model. Important results include the size and effectiveness of the heat exchanger, along with the mass flow rate required to deliver 10 W of cooling power.

Parameters:		
N = 20	D_{i} = 1 mm	D_{o} = 2 mm
P_{in} = 2 MPa	P_{out} = 0.1 MPa	$\dot{q}_{\mathrm{load}}$ = 10 W
$T_{\mathrm{h,in}}$ = 293 K	$T_{\mathrm{h,out}}$ = 190 K	
Results:		
$\dot{m}$ = 0.2 g/s	L_{helical} = 0.163 m	$L_{\mathrm{effective}}$ = 1.25 m
ε = 0.82		

Per the results of this simulation, the effective length of a 2 mm outer diameter tube-in-tube heat exchanger is 1.25 m. However, if this tube-in-tube heat exchanger were to be wound in a helix with a total outer diameter of 1 cm, the total length of the heat exchanger becomes just 0.163 m. These results suggest that it is possible for a ceramic cryosurgical probe to deliver 10 W of cooling at 170 K, while remaining a reasonable size. Along with the results presented in Table 2, Figure 5 shows the temperature and pressure profiles of the heat exchanger.

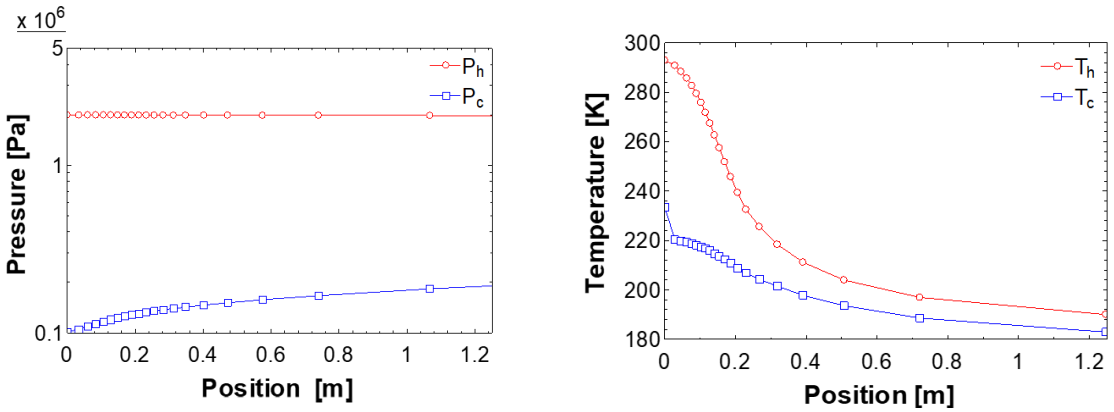

Figure 5. The (a) pressure and (b) temperature profiles of each side of the heat exchanger resulting from the numerical model. The pressure profile shows that most of the pressure drop occurs through the expansion valve, and not through the heat exchanger itself.

4. Conclusion

This paper reports the initial results of a thermal modelling effort to characterize the performance of a cryosurgical probe composed of MRI-compatible, that is non-metallic, materials. The model for a simple concentric tube recuperative heat exchanger includes the pressure and temperature dependent properties of an optimized gas mixture, as well as heat transfer and friction factor correlations for single- and two-phase flow, along with a mechanism to identify the regions associated with the two types of flow. In its present simple geometric form, the required length enables a reasonable size, in the form of a helically wound tube, to fit within the proximal end of a cryoprobe handle. A cooling power of 10 watts at 170 K is achieved with a mass flow rate of 0.2 g/s. Although the results of this simulation point towards a helically shaped heat exchanger, the fluid flow correlations used to arrive at that conclusion were developed for general two-phase or single-phase turbulent pipe flow. Further work to improve this model includes optimizing heat exchanger geometry to further reduce its size, developing a gas mixture that is absent of flammable hydrocarbons, and incorporating fluid flow correlations that more accurately represent helical flow channels.

Nomenclature

A_c	Cross sectional area (m^2)	T	Temperature (K)
Δh_T	Maximum minimum isothermal enthalpy change (J/kg)	UA	Conductance (W/K)
D_i	Inner tube diameter (m)		
D_o	Outer tube diameter (m)	*Greek*	
$\dot{C}_{min}$	Minimum conductance rate (W/K)	ε	Heat exchanger effectiveness

h	Specific enthalpy (J/kg)	γ	Axial conduction parameter
$\bar{h}$	Heat transfer coefficient (W/m^2-K)		
k_{zr}	Thermal conductivity of zirconium (W/m-K)	*Subscripts*	
L	Sub-heat exchanger length (m)	ac	Axial conduction
$\dot{m}$	Mass flow rate (kg/s)	i	Index of sub-heat exchangers
N	Number of sub-heat exchanger partitions	h	Heat exchanger hot side
$\dot{q}$	Total heat transferred by the heat exchanger (W)	c	Heat exchanger cold side
$\dot{q_d}$	Rate of heat transfer per sub-heat exchanger (W)	nac	No axial conduction
$\dot{q}_{\mathrm{load}}$	Cooling capacity, heat load (W)	cond	Conduction
R	Thermal resistance (K/W)	conv	Convection

References

[1] Harter R 2017 Series a executive summary (Middleton: Marvel Medtech, LLC) www.marvelmedtech.com
[2] Klein S 2019 EES-Engineering Equation Solver
[3] Skye H and Pfotenhauer J 2018 Joule thompson cryocoolers and cryoablation *Applications of Cryocoolers*
[4] Longsworth R 1994 Cryo-probe US Patent 5452582
[5] Detlor J, Pfotenhauer J and Nellis G 2017 Mixture optimization for mixed gas joule-thomson cycle *IOP Conf. Series: Materials Science and Engineering* **278** 012045
[6] Detlor J, Pfotenhauer J, and Nellis G 2018 Experimental investigation of mixture optimization for mixed joule-thomson cycle *Cryocoolers 20* (Boulder: ICC Press)
[7] Lemmon E, Huber M, and McLinden M 2013, Nist standard reference database 23: reference fluid thermodynamic and transport properties-refprop version 9.1 *National Institute of Standards and Technology*
[8] Nellis G and Klein S 2009 *Heat Transfer* (Cambridge; New York: Cambridge University Press) chapter 8 p 916
[9] Gnielinski V 1976 New equations for heat and mass transfer in turbulent pipe and channel flow *Int. Chem. Eng.* **16** 359–68
[10] Zigrang D and Sylvester N 1982 Explicit approximations to the solution of colebrook's friction factor equation *American Institute of Chemical Engineering Journal* **28** 514–15
[11] Shah M 1982 Chart correlation for saturated boiling heat transfer: equations and further study *ASHRAE Transactions* **88** 185–86
[12] Dobson M and Chato J 1998 Condensation in smooth horizontal tubes *Journal of Heat Transfer* **120** 193–213
[13] Ould Didi M, Kattan N and Thome J 2002 Prediction of two-phase pressure gradients of refrigerants in horizontal tubes *International Journal of Refrigeration* **25** 935-47